Tree top detection using local maxima filtering: a parameter sensitivity analysis

Jean-Matthieu Monnet, Eric Mermin, Jocelyn Chanussot, Frédéric Berger

Silvilaser 2010
September 14th - 17th
Freiburg, Germany

Tree top detection using local maxima filtering: a parameter sensitivity analysis

Jean-Matthieu Monnet*†, Éric Mermin†, Jocelyn Chanussot‡ & Frédéric Berger†

†UR EMGR, Cemagref, France
‡Gipsa-Lab, Grenoble Institute of Technology, France

The sensitivity of a treetop detection algorithm is investigated by automated evaluation of detection performance for several parameter combinations. The algorithm consists in digital elevation models computation, morphological filtering, Gaussian smoothing and local maxima extraction and selection. The analysis is performed on three field plots located in the French Alps. One is a Norway spruce stand while the two others are dominated by Silver fir and European beech. Detection rates above 42.9% are achieved with less than 4.1% of false positives. Even though some similarities exist regarding resolution and morphological filtering, optimal settings determined on one plot performed uncertainly on the others. Besides, optimised parameters may depend on both the laser data — mainly point density — and on the forest structure and species.

1. Introduction

In French mountainous forests, timber harvesting is economically sustainable only in areas where tree density and individual volume result in sufficient standing value. Indeed, topographical constraints increase both harvesting and transport costs. In practical terms, silvicultural operations are reduced to rare operations designed to maintain stand structure and made profitable thanks to the felling of very large trees (Ancelin *et al.* 2006). However, there is a renewed interest in mountainous areas in order to exploit woody renewable resources and preserve the ecological and social functions of forests. Unfortunately, stand characteristics information required for efficient stand management is frequently absent or outdated.

Airborne laser scanning (ALS) is a remote sensing technique whose applications for forest inventory have been widely investigated in the past fifteen years. In particular, numerous studies have shown its efficiency for single tree identification (Persson *et al.* 2002, Brandtberg *et al.* 2003, Popescu and Wynne 2004, Chen *et al.* 2006, Kwak *et al.* 2007, Heurich 2008). Usual methods rely on the computation of raster elevation models which are then filtered by image processing techniques to extract tree tops and delineate tree crowns. Several algorithms have been proposed and tested on particular forest contexts. Such techniques are of high interest for planning silvicultural and harvesting operations in mountainous forests. However, when dealing with large scale forest inventory, few calibration plots and little time for algorithm parametrisation are available. Hence the need to control the robustness of algorithms to parameters and input data.

The objective of this study is to perform an exploratory evaluation of the sensitivity of a basic tree top detection algorithm to parametrisation. Parameters influence is assessed by automatically evaluating detection performance for a high number of combinations. Optimum settings obtained on three plots are then cross evaluated to test their robustness.

*corresponding author. Email: jean-matthieu.monnet@cemagref.fr

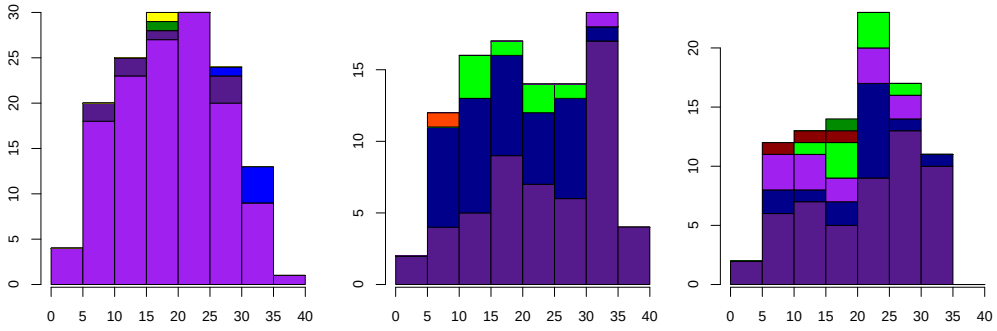

(a) Plot 1 *(b)* Plot 2a *(c)* Plot 2b

Figure 1. Height distribution of trees inventoried in the three test plots (frequency in percent as function of height classes in metres). Colours refer to tree species (■ *Abies alba*, ■ *Picea abies*, ■ *Fagus sylvatica*, ■ *Larix decidua*, ■ *Acer pseudoplatanus*, ■ *Betula sp.*, ■ *Prunus avium*, ■ *Ilex aquifolium*, ■ *Sorbus aucuparia*).

2. Material

2.1 *Field data*

The two forest stands investigated in this study are located in the French Alps. Plot 1 is an irregular stand dominated by Norway spruce (*Picea abies*) and located in the Chamonix valley (45°56'16"N, 06°53'55"E, altitude 1140 m). It was originally established to test new silvicultural strategies designed to improve mountainous stands stability and resilience (Mermin and Renaud 1996). The 0.25 ha square plot was first inventoried in 1994. The area was divided into squares with markers positioned every 12.5 m with a tape measure, a clinometer and a compass. Trees with diameter at breast height (DBH) larger than 7.5 cm had their positions to the nearest marker recorded with the same instruments. Plot corners were georeferenced using a Trimble GPS Pro XRS receiver. On June, 2nd 2009, the plot inventory was updated. DBH and tree heights were measured with a tape and a Vertex III hypsometer. 147 live trees were inventoried, with a majority of Norway spruce (89.8% of stems). Other species are silver fir (*Abies alba*, 5.4%), European larch (*Larix decidua*, 3.4%) and deciduous trees (1.4%). Figure 1(a) displays the distribution of tree heights on the plot.

Plot 2 is a study area initially used for real-size rockfall experiments (Dorren *et al.* 2006), located at Vaujany (45°12'07"N, 06°03'00"E, altitude 1280 m). It is an irregular stand dominated by Silver fir (*Abies alba*) with a deciduous understory. In 2001 twelve markers were positioned in the hillside. They were georeferenced using a Trimble GPS Pro XRS receiver. It is noteworthy that plot boundaries were not previously delimited, which resulted in an irregular shape. Trees with a DBH larger than 7.5 cm had their positions to the nearest marker recorded with a clinometer and a compass mounted on a tripod and with a laser rangefinder. On May, 12th 2009, the plot inventory was updated. DBH and tree heights were measured with a tape and a Vertex III hypsometer. For the purposes of this study, the plot is divided into two subplots. In the upper part of the study area (subplot 2a, 0.33 ha), 98 live trees were measured. Silver fir and European beech (*Fagus sylvatica*) are dominant (respectively 55.1 and 35.7% of the stems). Sycamore maples (*Acer pseudoplatanus*) are also encountered (7.1%), as well as Norway spruce and European holly (*Ilex aquifolium*) with 1% each. 92 live trees were inventoried in the lower part (plot 2b, 0.34 ha), with a majority of Silver fir (56.5%). European beech (16.3%) and Norway spruce (14.1%) are also present. The remaining stems are sycamores (8.7%) and other deciduous trees. Tree height distributions are shown on figure 1.

Table 1. Laser scanner acquisition parameters.

Plot number	1	2
Flight year	2007	2008
Wavelength (nm)	1550	1550
Pulse repetition rate (kHz)	200	200
Scan frequency (Hz)	104.4	73.3
Half scan angle (°)	30	30
Flight height (m)	550	500
Laser footprint (m)	0.29	0.27
Theoretical point spacing (m)	0.45	0.29
Final echo density (m^{-2})	7.8	36.6

2.2 *Laser data*

Laser data was acquired with a fullwave RIEGL LMS-Q560 scanner. Acquisition parameters are summarised in table 1. Echoes were extracted from the binary acquisition files and georeferenced with the RIEGL software suite. The contractor also classified the resulting point cloud into ground and non-ground echoes using the TerraScan software, which implements an algorithm based on iterative surface reconstruction by triangulated irregular network (Axelsson 2000). Plot 2 is located within the overlap of two adjacent flight strips which resulted in a high echo density (36.6 m^{-2}) whereas point cloud density was 7.8 m^{-2} for plot 1.

3. Methods

3.1 *Workflow*

For each test plot, the input data are the classified point cloud (easting, northing, altitude, classification,) and the inventoried trees list (easting, northing, height). Each step of the sequential procedure is explained in the following sections:

- calculation of the raster images from the point cloud,
- image processing with morphological and Gaussian filters,
- maxima extraction and selection with variable window size,
- performance assessment.

3.2 *Raster calculation*

The digital terrain model (DTM) is computed by bilinear interpolation of laser points classified as ground points over a regularly spaced grid of resolution res. The corresponding digital surface model (DSM) is based on the highest point recorded in each pixel. A basic, unfilled DSM ($DSM_{b,u}$) is calculated by affecting to each pixel the altitude of the highest point recorded in the cell. An interpolated, filled DSM ($DSM_{i,f}$) is calculated by bilinear interpolation of the highest points recorded in each cell, at the pixel centres. Void cells left in the basic DSM are interpolated from the neighbouring pixels to construct a filled basic DSM ($DSM_{b,f}$). On contrary pixels in $DSM_{i,f}$ without any laser points have their values erased to construct an unfilled interpolated DSM ($DSM_{i,u}$). Four corresponding crown height models (CHM) are computed by subtracting the DTM to the DSMs.

As plot extent was not previously delimited for plots 2a and 2b, raster masks are computed from the tree positions and heights. Buffers are constructed around each tree and merged. Remaining holes are filled by morphological closing with a 6 m radius structuring element. The previous external border is then reconstructed by morphological reconstruction. This procedure is designed to ensure that actual tree tops are located within the plot mask and therefore reduce border effects during the automated linking of detected maxima with inventoried trees. Indeed, due to

tree tilting and GPS position errors, tree tops may be located several metres away from the georeferenced tree trunks. Buffer radius r_t for a tree of height h_t (m) is $r_t = 2.1 + 0.14 \times h_t$ (see paragraph 3.5 for parameters explanation).

3.3 *Image processing*

The scanning pattern usually leads to several low or void pixels in the surface models, due to the irregular sampling and to the shading effect of trees at the borders of flight strips. This can be seen as a salt-and-pepper noise and be treated by several morphological filters: median, adaptive median, closing, reconstruction. Filter windows (half width) or structuring element (disk radius) sizes are $r_m \in \{0.25, 0.5, 0.75, 1, 1.5, 2\}$ (metres). Depending on the resolution res, sizes are approximated to the nearest integer number of pixels.

The final objective is to detect tree tops, i.e. the maxima of trees envelope. Local irregularities of branches and more generally of the canopy can be considered as high frequency noise. This can be filtered by Gaussian smoothing. Tested filter sizes in metres are $\sigma \in \{0, 0.1, 0.2, 0.3, 0.4, 0.5, 0.75, 1, 1.25, 1.5, 2, 3, 4\}$. A discrete approximation of the continuous filter is used.

3.4 *Maxima extraction and selection*

Maxima are extracted with a sliding filter of variable size. Pixel values in the resulting maxima image correspond to the half width (metres) of the biggest centred square window where the corresponding pixel is global maximum in the original image. The plot mask is then applied to the maxima image to set the values of all pixels outside the plot to zero.

At this stage there are high chances that some of the local maxima are not actual tree tops but vertical branches, dual apexes of deciduous trees... A maxima selection procedure based on a minimum height and on the relationship between a maxima height h_m and its distance to the nearest higher pixel d_m is performed. Maxima which do not fulfil the following inequalities are discarded.

$$\begin{cases} d_m \geq d_{min} + d_{prop} \times h_m \\ h_m \geq h_{min} \end{cases} \quad \text{with } (d_{min}, d_{prop}, h_{min}) \text{ the selection parameters}$$

Their values in the maxima image are set to zero. Tested parameters are $(d_{min}, d_{prop}) \in \{(0.5, 0), (0.75, 0), (1, 0), (1.5, 0), (1.75, 0), (2, 0), (2.25, 0), (2.5, 0), (1.5, 1/80), (1, 1/40), (2/3, 1/30), (10/25, 1/25), (0, 1/20)\}$ and $h_{min} \in \{0, 2.5, 5, 7.5, 10, 12.5, 15\}$.

The final list of selected maxima is extracted from the image. Maxima are assumed to be located at the centre of the pixels with non-zero values. Maxima heights h_m are estimated as the values of the corresponding pixels in the morphologically filtered image. Maxima distances to the nearest pixel of higher value d_m are the values in the maxima image.

3.5 *Performance assessment*

An automated procedure is used to link selected maxima to inventoried trees. It is assumed that GPS positioning planimetric error ϵ_{gps} is inferior to 1.5 m and that the slope of a tilted tree s_{tree} is inferior to 14% (value determined by measures performed on the 26 highest trees in plot 2). Height measures accuracy is estimated

to be $\epsilon_h = 15\%$. Under these asumptions, the limit matching distance between a selected maxima and a field tree top assumed to be vertically located at h_t metres above the GPS position of tree T is:

$$d_{max}(h_t) = \frac{\epsilon_{gps}}{\cos(s_{terrain})} + s_{tree} \times (\epsilon_h + 1) \times h_t$$

with $s_{terrain}$ the terrain slope. For each pair constituted of a tree T and a maxima M of respective heights h_t and h_m, a matching index $I_{T,M}$ is computed as the ratio of the distance between the assumed tree top and detected maxima, and $d_{max}(h_t)$.

$$I_{T,C} = \frac{d_{T,C}}{d_{max}(h_t)}$$

The potential pair with the lowest matching index is validated and the lists of remaining maxima and trees are updated before reiterating the procedure. Linking ends when all remaining values of $I_{T,C}$ are greater than 1.

For accuracy assessment a trade-off between the true positives ratio (percentage of correctly detected trees $R_{TP} = \frac{N_{TP}}{N}$) and false positives ratio (ratio of unlinked detected maxima to field trees number $R_{FP} = \frac{N_{FP}}{N}$) has to be found. It is assumed that for every five additional true positives, one false positive is tolerated. The accuracy score S is thus computed as:

$$S = (w \times R_{FP})^2 + (1 - R_{TP})^2 \qquad \text{with } w = 5$$

which corresponds to the squared euclidean distance to the perfect match ($N_{FP} = 0$ and $N_{TP} = N$) with the false positives ratio weighted by a factor 5.

All computations are performed using Matlab® and its Image Processing Toolbox. For each plot (1 and 2) and also for the subplots (2a and 2b) considered separately, all combinations of parameters (total number: 1381744) are tested and accuracy results recorded. To assess the precision of tree height estimation, linear models are fitted with field height as independent variable and maxima height as dependent variable.

4. Results

4.1 *Optimal settings*

The best scores and corresponding parameter settings for plots 1, 2 and subplots 2a and 2b are displayed in table 2. Detection rates above 42% are achieved with respectively 6, 2 and 2 false alarms for plots 1, 2a and 2b. These results are obtained with the smallest tested resolution ($res = 0.2$ m). A stronger morphological filtering is performed for the Vaujany subplots (2a and 2b) whereas maxima filtering is less selective. Indeed the best score is attained for several values of h_{min} and only maxima that are very close to their nearest higher pixel ($d_{min} = 0.5$ m) are removed. It is noteworthy that the optimum setting for the entire plot 2 is different from those of subplots 2a and 2b considered alone. Moreover, overall accuracy obtained in plot 2 is quite lower.

In figure 2, field heights of detected trees (h_t) ars plotted against corresponding maxima heights (h_m). Linear regressions show that on plot 1 tree heights are underestimated by about 1 meter (slope: 1.04 and intercept: 0.93 m). On the Vaujany site, heights of big trees are overestimated whereas small trees are slightly underestimated (slopes inferior to 0.91).

Table 2. Best detection results and corresponding parameter settings.

	Accuracy assessment			Height model		Morphological		Gaussian	Maxima selection		
Plot	Score	R_{TP}	R_{FP}	res	Model	Type	r_m	σ	h_{min}	d_{min}	d_{prop}
1	0.32	46.9	4.1	0.2	$CHM_{b,u}$	closing	0.4	0.3	7.5	1	0.025
2a	0.34	42.9	2.0	0.2	$DSM_{i,f}$	median	1	0.1	5-15	0.5	0
2b	0.32	44.6	2.2	0.2	$CHM_{i,u}$	median	0.8	1	0-7.5	0.5	0
2	0.39	38.9	2.6	0.2	$CHM_{b,i}$	median	1	0.1	12.5	0	0.05

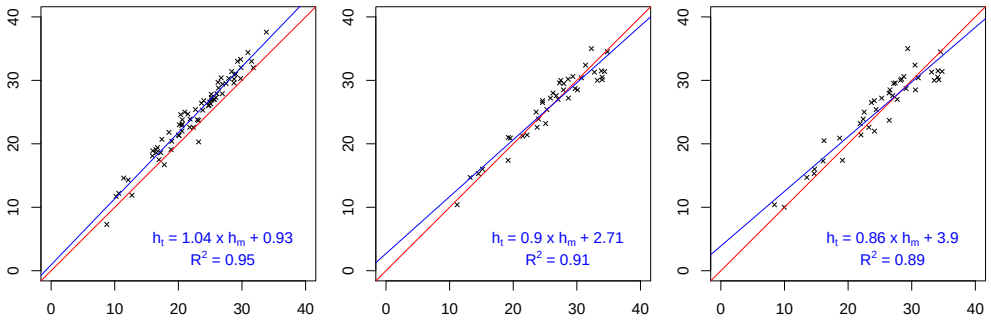

(a) Plot 1 *(b)* Plot 2a *(c)* Plot 2b

Figure 2. Field height h_t plotted against laser estimated height h_m for trees correctly detected in the three test plots. Red line corresponds to $y = x$. Blue line is linear regression of h_t against h_m. Corresponding detection settings and accuracy are displayed in table 2.

4.2 *Parameter sensitivity*

The effect of the various parameters on detection accuracy are displayed in figure 3. Due to the high number of combinations only the monotonically increasing border of the point groups envelopes are represented in the (R_{FP}, R_{TP}) plane, with $R_{FP} \leq 0.2$ and $R_{TP} \geq 0.2$. For plot 1, resolutions below 0.5 m pixel size give similar accuracy (figure 3(a)), whereas for plots 2a and 2b parameter combinations with higher resolutions allow better results. On plot 2a, filled DSMs seem well adapted (figure 3(b)), contrary to plots 1 and 2a where unfilled CHMs obtain slightly better accuracy.

The median filter performs well in all cases (figure 3(c)) and is particularly superior to other morphological filters when employed in plot 2a on a two metres wide square window. Gaussian filter does not seem to improve performance in this plot, whereas moderate smoothing (respectively with σ around 0.8 and 0.3 m) is advantageous for plots 1 (figure 3(d)) and 2a.

Maxima selection by height thresholds does not enhance detection performance. In plot 2a, maxima selection with a fixed radius distance to the nearest higher pixel brings improvement (figure 3(e)), whereas selection based on a radius proportional to maxima height performs better with the other plots (figure 3(f)).

4.3 *Stand sensitivity*

Table 3 shows the detection accuracy obtained on the test plots when the parameter setting is calibrated on another plot. Plot 1 parameters result in high false positives rate in the other plots. Plot 2a settings achieve the highest number of true positives, but with a relatively large number of false detections in plot 2b. Parameters of plot 2b perform poorly. Finally global settings for plot 2 yield an acceptable compromise between detection rate and false alarms in all plots.

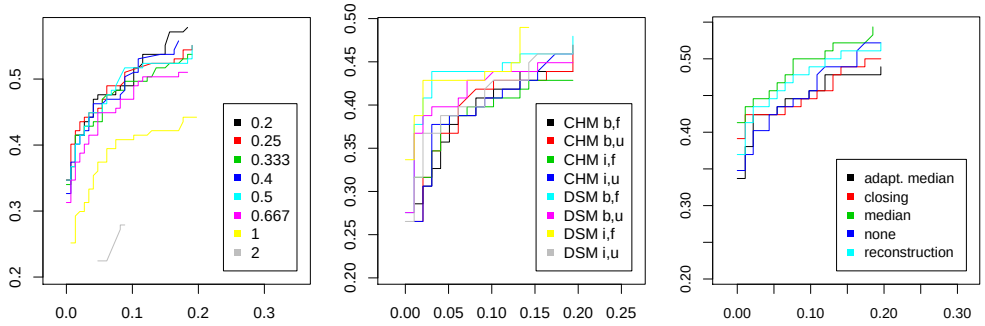

(a) Resolution (m, plot 1) *(b)* Input raster (plot 2a) *(c)* Morphological filter (plot 2b)

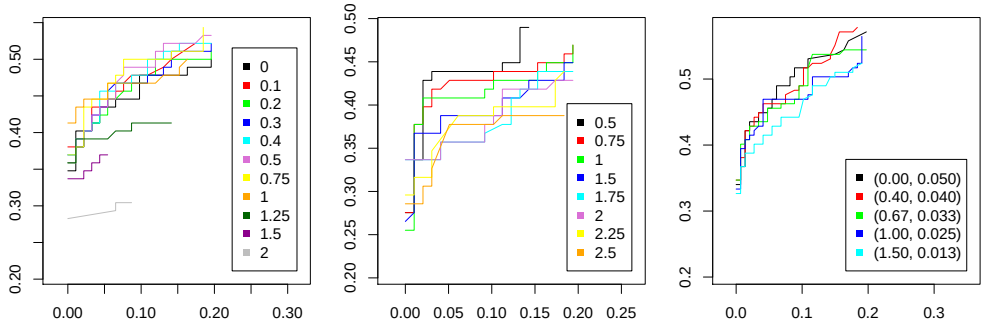

(d) σ (m, plot 1) *(e)* d_{min} (m, $d_{prop} = 0$, plot 2a) *(f)* (d_{min}, d_{prop}) (plot 1)

Figure 3. Plots in the (R_{FP}, R_{TP}) plane of the monotonically increasing envelopes of points groups obtained with various settings for a given parameter.

Table 3. Accuracy of optimal settings determined on one test plot when used on another plot. Triplets are constituted of true positives rate R_{TP} (%), false positives rate R_{FP} (%) and height RMSE (m) for detected trees.

Plot	Plot 1 settings			Plot 2a settings			Plot 2b settings			Plot 2 settings		
1	46.9	4.1	2.28	38.8	4.1	3.14	4.1	4.1	1.97	35.4	2.7	3.09
2	36.3	14.7	2.03	42.6	9.5	1.94	32.1	8.4	2.29	38.9	3.2	1.9
2a	31.6	15.3	1.93	42.9	2.0	2.09	20.4	14.3	2.35	36.7	1.0	1.94
2b	41.3	12.0	2.11	42.4	16.3	1.76	44.6	2.2	2.26	41.3	4.4	1.86

5. Discussion

Detection results are similar to those obtained by Heurich (2008) in richly structured forests in Bavaria, with 76.9% of the trees in the upper layer identified and 5.4% detection error. On plot 2, 65.4% (resp. 84.8%) of trees above 20 m (resp. 25 m) are identified with 2.6% of false positives. In the same study, 46.8% of trees in high altitude spruce plots were determined with only 0.8% false detection, which is close to results obtained on plot 1. However such comparisons must be handled with care due to differences in field protocols, detection methods and evaluation criteria.

Underestimation of tree heights in coniferous stands such as plot 1 is a common situation (Gaveau and Hill 2003). For mountainous areas, Hirata (2004) explained that the tilting of trees toward downslope results in an overestimation of tree height by scanner laser. Indeed, additional measures (data not shown) performed on the 26 taller trees in plot 2 show that the vertical distance between tree apex and ground is significantly greater than the vertical distance between tree apex and stem base (bias: 2.76 m, $p < 0.001$ in Student t-test).

Detection results obtained with settings calibrated on plots different from the tested plot show that in mountainous stands, algorithm performance highly de-

pends on the parametrisation. Trends in parameter sensitivity of the algorithm may be related to both laser scanner acquisition parameters and stand characteristics. In plot 1 laser point density is lower which may explain why resolutions of pixel size lower than 0.5 m do not bring any major improvement. Indeed, there is no additional information in the point cloud to be transferred to the raster elevation models, as most of the additional pixels are empty. Regarding other parameters, plot 1 and 2b display similar tendencies. Plot 2a singularities may be explained by the high proportion of deciduous trees. Indeed, hole filling during raster computations and median filtering may have more importance when dealing with irregular, concave crowns of beech than with those of spruce or silver fir. Besides, in mixed complex stands with tree collectives, relations between tree height, diameter and crown surface are not straightforward. This may explain why basic distance thresholds perform better than diameter-height relationships for maxima selection.

It turns out from this exploratory analysis that accuracy of a basic tree top detection algorithm requires careful parametrisation. A better hindsight would be acquired by testing the algorithm on other stands and with different laser data (hardware, acquisition parameters) and also by investigating the combined influence of parameters. To reduce the range of investigated values, some parameters such as optimal raster resolution may be roughly estimated from input data characteristics. For example, Chen *et al.* (2006) determine raster resolution from the point cloud density and variable window size for maxima selection from the prediction intervals of the tree height relationship with crown size. Construction of a robust, generic parameters setting is also of interest when processing newly acquired laser data with no prior knowledge on the forest stands.

6. Conclusion

The analysis of the parameters influence on tree top detection in two forest stands show that identification accuracy highly depends on algorithm settings. Besides, optimal values may be linked to input data such as laser points density or forest stand characteristics (structure and species).

In order to design a semi-supervised procedure for wide area single-tree based inventories in complex areas, further research is required to investigate how prior stand knowledge or preparatory tree identification with generic settings could help determine optimal detection parameters.

Acknowledgements

J.-M. Monnet held a doctoral fellowship from Cluster de Recherche Energies (région Rhône-Alpes, France).

References

Ancelin, P., Barthelon, C., Berger, F., Cardew, M., Chauvin, C., Courbaud, B., Descroix, L., Dorren, L., Fay, J., Gaudry, P., Gauquelin, X., Joud, D., Loho, P., Mermin, É., Plancheron, F., Prochasson, A., Rey, F., Rubeaud, D. and Wlérick, L., 2006, *Guide des sylvicultures de montagne: Alpes du Nord Françaises.*

Axelsson, P., 2000, DEM generation from laser scanner data using adaptive TIN

models. In *Proceedings of the XIXth ISPRS Congress, IAPRS*, XXXIII, pp. 110–117.

Brandtberg, T., Warner, T.A., Landenberger, R.E. and McGraw, J.B., 2003, Detection and analysis of individual leaf-off tree crowns in small footprint, high sampling density lidar data from the eastern deciduous forest in North America. *Remote Sensing of Environment*, **85**, pp. 290–303.

Chen, Q., Baldocchi, D., Gong, P. and Kelly, M., 2006, Isolating individual trees in a savanna woodland using small footprint lidar data. *Photogrammetric Engineering and Remote Sensing*, **72**, pp. 923–932.

Dorren, L.K.A., Berger, F. and Putters, U.S., 2006, Real-size experiments and 3-D simulation of rockfall on forested and non-forested slopes. *Natural Hazards And Earth System Sciences*, **6**, pp. 145–153.

Gaveau, D.L.A. and Hill, R.A., 2003, Quantifying canopy height underestimation by laser pulse penetration in small-footprint airborne laser scanning data. *Canadian Journal of Remote Sensing*, **29**, pp. 650–657.

Heurich, M., 2008, Automatic recognition and measurement of single trees based on data from airborne laser scanning over the richly structured natural forests of the Bavarian Forest National Park. *Forest Ecology and Management*, **255**, pp. 2416–2433.

Hirata, Y., 2004., The effects of footprint size and sampling density in airborne laser scanning to extract individual trees in mountainous terrain. In *International Archives of Photogrammetry, Remote Sensing and Spatial Information Sciences XXXVI (Part 8/W2)* pp. 102–107.

Kwak, D.A., Lee, W.K., Lee, J.H., Biging, G.S. and Gong, P., 2007, Detection of individual trees and estimation of tree height using LiDAR data. *Journal of Forest Research*, **12**, pp. 425–434.

Mermin, É. and Renaud, J., 1996, Installation de placettes permanentes dans les forêts résineuses des Alpes du Nord : objectifs, méthode, résultats. Technical report, Cemagref.

Persson, Å., Holmgren, J. and Soderman, U., 2002, Detecting and measuring individual trees using an airborne laser scanner. *Photogrammetric Engineering and Remote Sensing*, **68**, pp. 925–932.

Popescu, S. and Wynne, R., 2004, Seeing the trees in the forest: using lidar and multispectral data fusion with local filtering and variable window size for estimating tree height. *Photogrammetric Engineering and Remote Sensing*, **70**, pp. 589–604.